Thermal insulation of walls and roofs by PCM: modeling and experimental validation

Kamal A. R. Ismail, J. N. Castro, Fatima A. M. Lino

Abstract— **In hot and tropical countries external walls and roofs receive solar radiation absorbing part of it and transmitting a substantial part to the internal ambient provoking thermal discomfort. In cold climate heat is usually lost to the external ambient and again causing thermal discomfort. In both cases the thermal energy load is increased. For these reasons many studies were dedicated to investigate techniques for improving the thermal performance of walls and roofs. One of the most viable techniques is the use of PCM as thermal insulation filler that increases the thermal inertia of the component at relatively low cost and without substantial increase of weight. The formulation of the problem of the PCM composite wall is based on one dimensional pure conduction model for the PCM and the walls. The numerical solution involves moving grid for the PCM. The computational grid was optimized to eliminate grid size effects. The model was extended to treat the roof problem. The numerical predictions were compared with experimental results and reasonably good agreement was found. Additional numerical and experimental results were presented and discussed.**

Index Terms— **Energy reduction in buildings, passive thermal comfort, PCM walls, PCM roofs, solar heat gain.**

I. INTRODUCTION

Thermal storage plays an important role in building energy conservation. This is greatly accomplished by the incorporation of latent heat storage in building components. This technique is very attractive because of the high storage density with small temperature swing. Thermal energy storage in walls, ceilings and floors of buildings may be enhanced by embedding PCM within these construction elements. Increasing the thermal storage capacity of a building can decrease the internal temperature oscillations.

The use of PCMs in buildings provides the potential for a better indoor thermal comfort and lower energy consumption due to the load reduction/shifting. Hence a good knowledge of the dynamic energy performance of buildings using PCM is essential for building designers to better understand building temperature response, enhancing indoor environmental quality and overall energy efficiency of buildings.

Solar walls have been studied for decades as a way of heating building from a renewable energy source due to their high storage capacity. However, this increases their weight and volume, which limits their integration into existing building. To alleviate this problem, storage mass is replaced by phase change materials which allow storing a large amount of energy in a small volume and permits retrofitting through use of light prefabricated module. In this type of application the PCM must have high thermal conductivity to have a significant reduction of the building energy consumption. Another important factor is that the calculated PCM mass must be sufficient to ensure that the PCM does not melt completely before the sunset and does not re-solidify completely before the sunrise.

The same technology of incorporating PCM in walls can be used for PCM roofs and floors to enhance thermal comfort in the interior space of a building and economize energy consumption.

Bernard et al. [1] reported the results of a comparative experimental study on PCM and sensible heat thermal walls. The energy gain of the PCM wall and the internal temperature variations were compared with those of the concrete wall. It was found that the PCM wall had better thermal performance and a mass of about 1/12 the mass of the concrete wall, thus suitable for retrofit.

Ismail and Castro [2] presented the results of a numerical and experimental study of walls and roofs filled with PCM to achieve passive thermal comfort. The thermal model is one-dimensional controlled by pure conduction. Comparison between the simulation results and the experiments indicated good agreement. Further analysis indicated that the concept could effectively help in reducing the electric energy consumption, improve the energy demand pattern and reduce greenhouse emissions.

Carbonari et al. [3] used a finite element numerical algorithm validated with experimental results for the simulation of the problem of heat transfer with phase change. Good agreement was found between the numerical predictions and experiments.

Tyagi and Buddhi [4] presented a comprehensive review of possible methods for heating and cooling in buildings such as PCM Trombe wall, PCM wallboards, PCM shutters, PCM building blocks, air-based heating systems, floor heating, ceiling boards, etc. All these systems have good potential for reducing the energy demand of heating and cooling in buildings.

It has been demonstrated that increasing the thermal storage capacity of a building can enhance human comfort by

Ismail, K.A.R., Full Professor, State University of Campinas (UNICAMP), Faculty of Mechanical Engineering, Energy Department, Mendeleiev street, 200, Cidade Universitária "Zeferino Vaz", Barão Geraldo, Campinas, SP, Brazil, Postal Code 13083-860, Phone: +55 19 35213376, Fax +55 19 32893722.

Castro, J.N., PhD. Department of Energy, Faculty of Mechanical Engineering, State University of Campinas, Mendeleiev street, 200, Cidade Universitária "Zeferino Vaz", Postal Code 13083-860, Campinas (SP), Brazil. Phone: +55 19 35213376.

Lino, F.A.M., PhD, State University of Campinas (UNICAMP), Faculty of Mechanical Engineering, Energy Department, Mendeleiev street, 200, Cidade Universitária "Zeferino Vaz", Barão Geraldo, Campinas, SP, Brazil, Postal Code 13083-860, Phone: +55 19 35213376

decreasing the frequency of internal air temperature swings, temperature close to the required temperature as in [5, 6, 7].

In conventional buildings thermal mass is a permanent building characteristic and not necessarily optimum in all operational conditions. Hoes et al. [8] proposed a concept that combines the benefits of buildings with low and high thermal mass by applying hybrid adaptable thermal storage systems and materials to a lightweight building. Calculations show heating energy demand reductions of up to 35% and increased thermal comfort compared to conventional thermal mass concepts.

Thermal mass combined with other passive strategies can play an important role in buildings energy efficiency, minimizing the need of space-conditioning mechanical systems. However, the use of lightweight materials with low thermal mass is becoming increasingly common. PCM can add thermal benefits to lightweight constructions as in [9, 10, 11, 12, 13, 14].

Sajjadian et al. [15] presented a method to assess the effect of PCMs on thermal comfort and energy consumption in UK dwellings in summer months. It was shown that appropriate levels of PCM, with a suitable incorporation mechanism into the building construction, can reduce discomfort and cooling energy loads.

Roofs also received a special attention and dedicated experimental, numerical and full scale experimental studies to investigate their contribution to the thermal comfort of the occupants of a building. Saman et al. [16] analyzed the thermal performance of a roof integrated solar heating system developed for space heating of a home. Warm air delivered by a roof integrated collector is passed through the spaces between the PCM layers to charge the storage unit. The results are compared with a previous analysis and reasonably good agreement was found.

Other additional studies on modeling, numerical treatment and experiments involving small scale and full scale models were also reported as in [2, 17, 18, 19, 20, 21].

The objective of this paper is to demonstrate the viability of using PCM incorporated in walls and roofs to increase the thermal inertia of the system and reduce the temperature variations and energy losses. The models were solved numerically and the results were validated against experimental results. The comparisons showed reasonably good agreement confirming the potential of the concept in reducing energy gains and maintaining thermal comfort in buildings.

II. MODELING OF THE PCM WALL AND ROOF

A. Wall with PCM

The composite wall is made of conventional construction material having a total thickness as a conventional wall and with the space between the walls filled with PCM as shown in Fig. 1. The composite wall is subject to solar radiation on the external side, heat conduction in the first solid wall, conduction in the PCM layer, conduction in the second wall and convection on the surface of the second wall facing the internal ambient. In the model formulation convection in the PCM liquid phase, interface resistance between the wall and PCM, and edge effects are neglected.

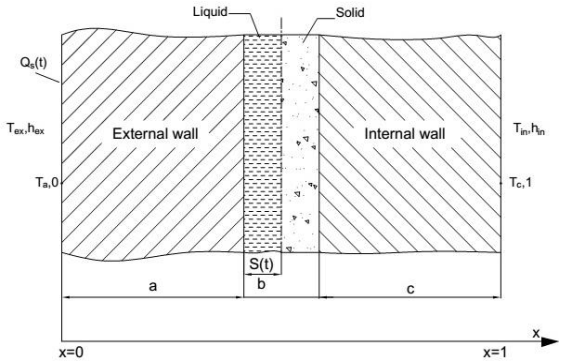

Fig. 1 Layout of the PCM wall problem with relevant data.

Additional assumptions include constant physical properties ,constant convection heat transfer coefficients, and that the variation of the external wall temperature is according to the energy balance between the incident radiation and the involved heat transfer mechanisms, that is, conduction, convection and radiation.

Considering that there is no viscous dissipation, no compressibility and constant specific mass, one can write the energy equation in the form:

$$\frac{\partial T_i}{\partial t} = \alpha_i \nabla T_i \qquad (1)$$

Where $i = a,b,c$

a = external wall, b = PCM, c = internal wall.

Considering the symmetry of the temperature field along the length and height of the wall, and that the physical properties are uniform and independent of the temperature, equation (1) is reduced to Fourier equation as

$$\frac{\partial T_i}{\partial t} = \alpha_i \frac{\partial^2 T_i}{\partial x^2} \qquad (2)$$

Where $i = a,b,c$

Equation (2) can be applied to the external wall, PCM and the internal wall.

A) External wall

For the external wall, one can write

$$\frac{\partial T_a}{\partial t} = \alpha_a \frac{\partial^2 T_a}{\partial x^2} \qquad 0 \le x \le a \qquad (3)$$

The boundary conditions are

a) The external wall face, x = 0 , the energy balance yields

$$-k_a \left.\frac{\partial T_a}{\partial t}\right|_{x=0} = h_{ex}\left(T_s - T_{a(x=0)}\right) \quad (4)$$

Where

$$T_s = \frac{\alpha_{sol} Q_s(t) + h_{ex} T_{ex} - \varepsilon \Delta R}{h_{ex}} \quad (5)$$

$Q_s(t)$ = Solar insulation.

By using Hottel's model [22] for the direct radiation, the model due to Liu and Jordan [23] of the diffuse radiation and the available climatic data it is possible to simulate the global radiation on a horizontal surface, the solar temperature and the temperature of the external ambient.

T_{ex}= Hourly external air temperature for the adopted days of the month, determined according to ASHRAE [24] and the regional climatic data.

h_{ex}= External convection coefficient obtained from [24].

$\varepsilon \Delta R$ = Long wave length resultant radiation obtained from [24].

b) At x = a, it is possible to have one of the following conditions according to the situation,

b1) Sub cooled PCM at temperature below its phase change temperature

$$k_a \left.\frac{\partial T_a}{\partial x}\right|_{x=a} = k_s \left.\frac{\partial T_s}{\partial x}\right|_{x=a} \quad (6)$$

b2) PCM at the phase change temperature and with heat flux to form a thin layer of liquid PCM

$$k_a \left.\frac{\partial T_a}{\partial x}\right|_{x=a} = \rho\lambda \frac{d_s(t)}{dt} + k_a \left.\frac{\partial T_a}{\partial x}\right|_{x=a} \quad (7)$$

b3) PCM in the liquid phase

$$k_a \left.\frac{\partial T_a}{\partial x}\right|_{x=a} = k_\ell \left.\frac{\partial T_\ell}{\partial x}\right|_{x=a} \quad (8)$$

PCM region

Due to phase change process, one has three sub regions, that is, liquid phase, fusion interface and solid phase.

For the liquid and solid phase, one can write:

$$\frac{\partial T_j}{\partial t} = \alpha_j \frac{\partial^2 T_j}{\partial x^2} \quad (9)$$

Where

j= ℓ = liquid at a < x < a + s (t)
j = s = solid at a + s (t) < x < a + b

For the interface position $x = a + s(t)$ and from the energy balance

$$k_s \frac{\partial T_s}{\partial t} - k_l \frac{\partial T_l}{\partial t} = \rho\lambda \frac{ds(t)}{dt} \quad (10)$$

The boundary conditions for these situations are:

a) At x = a, the boundary conditions are the same as in item (b) in the first region.

b) At $x = a + s(t)$ eq. (10) is the boundary condition together with

$$T_\ell = T_s = T_m \quad (11)$$

c) At $x = a + b$, two boundary conditions are possible depending on the localization of the phase change interface.

c1) As long as there is a solid phase

$$k_s \left.\frac{\partial T_s}{\partial x}\right|_{x=a+b} = k_c \left.\frac{\partial T_c}{\partial x}\right|_{x=a+b} \quad (12)$$

c2) When there is only liquid phase

$$k_l \left.\frac{\partial T_l}{\partial x}\right|_{x=a+b} = k_c \left.\frac{\partial T_c}{\partial x}\right|_{x=a+b} \quad (13)$$

Internal wall

$$\frac{\partial T_c}{\partial t} = \alpha_c \frac{\partial^2 T_c}{\partial x^2}, \text{ valid for } a+b<x<a+b+c \quad (14)$$

The boundary conditions are:

a) At x = a + b , the same as those of case (c) in the second region;

b) At x = a + b + c

$$-k_c \frac{\partial T_c}{\partial x} = h_{in}\left(T_{c(x=a+b+c)} - T_{in}\right) \quad (15)$$

T_{in} is the internal ambient temperature kept constant.

The proposed model is solved numerically by the finite difference technique in the regions where there is no moving interface. In the phase change region the numerical solution was done using moving grid as suggested by Murray and Landis

[25]. Numerical tests were realized to establish the grid size which makes the results independent of the grid size.

B. Roof with PCM

In this case the roof is built using conventional construction materials with a layer of PCM. The PCM roof is subject to solar radiation on the external face, heat conduction in the PCM layer, conduction in the concrete and convection on the internal surface facing the internal ambient as shown in Fig. 2. Convection in the PCM liquid phase, the contact resistance between the concrete slab and PCM, and edge effects were neglected. It is assumed that the physical properties and the convection heat transfer coefficients are constant. It is also assumed that the variation of the external wall temperature is according to the energy balance between the incident radiation and the involved heat transfer mechanisms, that is, conduction, convection and radiation.

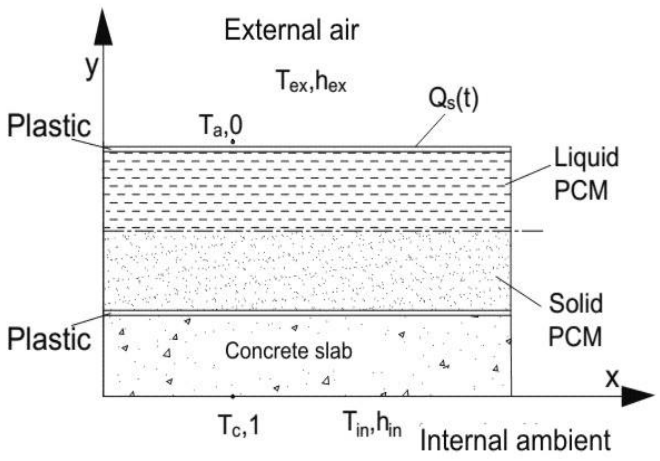

Fig. 2. Layout of the PCM roof problem showing the relevant data.

In a similar manner the model is constructed following the same steps as in the case of the wall and putting the boundary conditions according to the position across the composite roof. The details of the model are not presented for the sake of brevity.

A similar computer program is written in FORTRAN and solved numerically by finite differences in the regions where there is no moving interface. In the phase change region the numerical solution was done using moving grid as suggested by [25]. Numerical tests were realized to optimize the grid size.

III. Experiments on PCM wall and roof

To validate the experimental model and the numerical predictions an experimental installation was constructed as shown in Fig. 3, using conventional construction materials. A small room has a conventional roof and conventional north-facing wall. The second room has a PCM movable wall and roof. The north-facing wall and the roof were designed to be movable to permit testing walls and roofs of different configurations. The composite wall is formed of two parallel walls constructed from conventional bricks and the spacing in between is filled with PCM. The PCM is contained in plastic bags arranged in a layer of 2.0 or 4.0cm thickness. Both walls , the conventional and the PCM wall, were instrumented with calibrated thermocouples placed across the wall thickness and across the PCM layer.

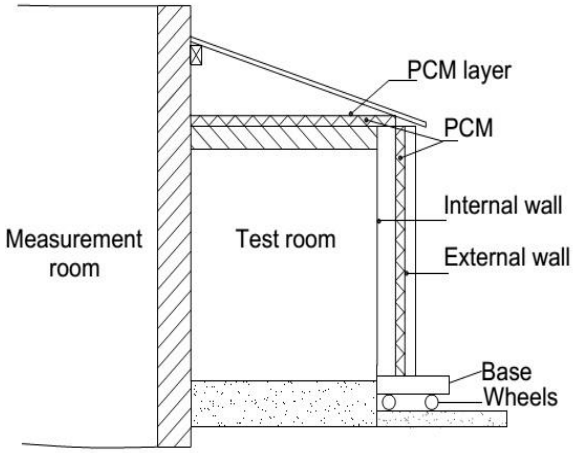

Fig. 3 The PCM wall and roof testing facility.

The two roofs were also constructed from conventional material, one fixed permanently in place while the other is movable covered with a layer of PCM contained in plastic bags. The PCM used is the same as that used in the wall assembly. Temperatures were measured by calibrated thermocouples poisoned across the roof and the PCM layer. Thermocouples were also fixed on the walls and roof internal and external surfaces. A general section of the test facility is shown in Fig. 3.

The structure, details and overall dimensions of the moving PCM wall are shown in Fig. 4a while Fig. 4b shows the details of the PCM moving roof.

The bricks used in the simulation are the same as normally used in constructing residences and their properties and dimensions are presented following

- Dimensions: 20 x 10 x 5 cm;
- Thermal conductivity = 0.7 W/m. K;
- Specific mass = 1600 kg/ m^3 , and
- Specific heat = 840 J/kg. K.

The PCM used in this study is a mixture of commercial polyethylene glycol (available in the laboratory at the time) known commercially as ATPEG or PEG. We formulated a mixture of PEG 600 whose fusion temperature is 23 ^oC and PEG 1000 whose temperature range is 35-36 ^oC. Different mixtures of PEG 1000 with PEG 600 were made and tested to determine the desired fusion temperature range. It was found that the mixture ratio of one part of PEG 1000 to four parts of PEG 600 gave a fusion temperature range of 21.5-25.5 ^oC which is the temperature range for this study.

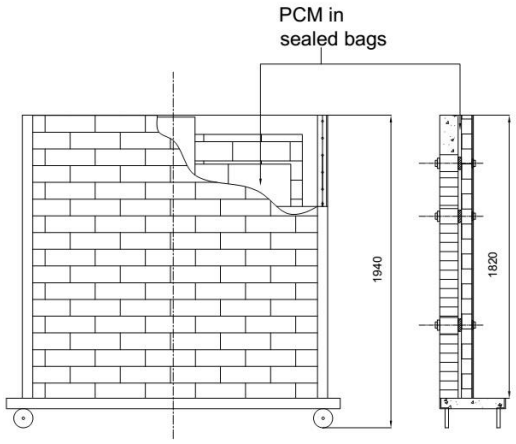

(a) Details of PCM wall.

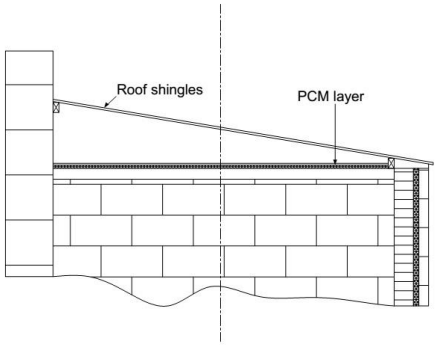

(b) Details of PCM roof.

Fig. 4 Sections of the test facility showing details of the PCM wall and roof.

For this mixture additional tests were realized to determine the latent heat of fusion and the specific heat by using DSC calorimetry and the result is shown in Fig.5a.

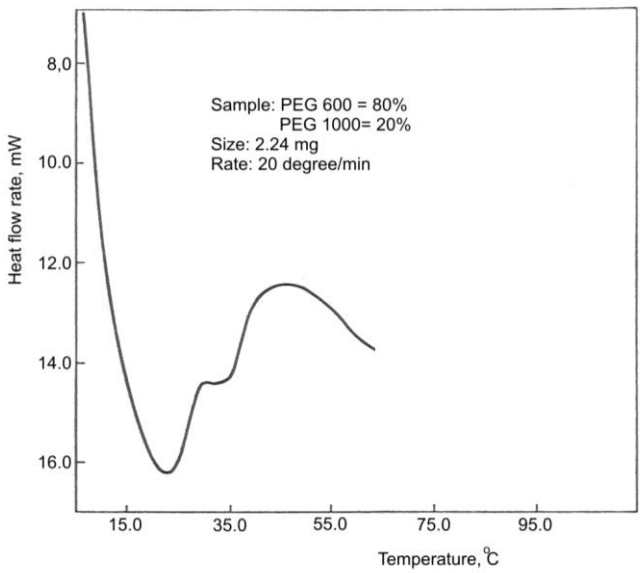

Fig.5a. Fusion diagram of the mixture 4:1 PEG 600 and PEG 1000.

The following results were found:

- Latent heat of fusion = 150.5 kJ/kg
- Specific heat of solid at 20 ^{o}C = 1.64 kJ/kgK
- Specific heat of liquid at 40 ^{o}C = 1.87 kJ/kgK

The specific mass of the mixture was determined by measuring the mass and volume at different temperatures in the case of the liquid phase and the results are shown in Fig. 5b. In the case of the solid phase at temperature 20 ^{o}C the specific mass is 1135.4 kg/m^3.

The thermal conductivity was measured by the hot plate type apparatus for the determination of thermal conductivity of liquid. The thermal conductivity at 40 ^{o}C is 0.53 W/mK.

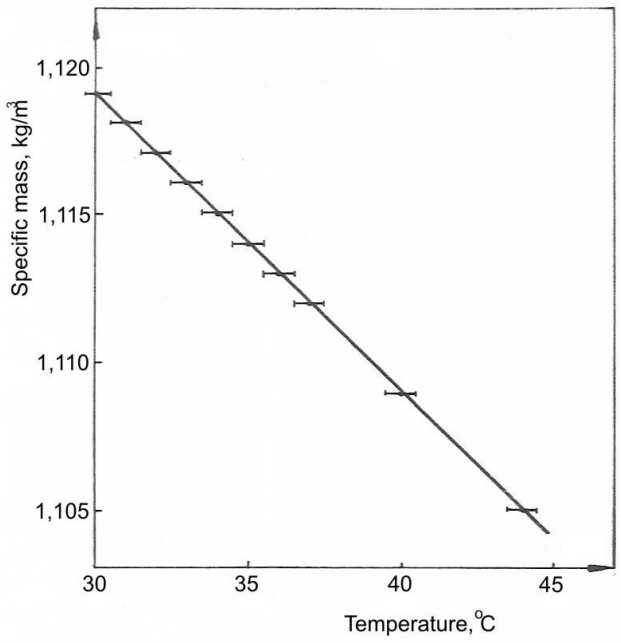

Fig. 5b. Variation of the specific mass of the PCM mixture (4:1 PEG 600 in PEG 1000) with temperature.

IV. RESULTS AND DISCUSSION

Fig. 6 shows the transient temperature variation across a conventional wall composed of two half brick laid side by side. The solar radiation incident on the right side of the graph, heats up the external side which passes over this heat to the internal ambient air by conduction and convection causing its temperature to increase progressively. At night the external temperature drops down and consequently, heat is transferred in the opposite direction that is to the external ambient causing the internal ambient temperature to decrease too.

If a layer of PCM is inserted between the bricks the temperature distribution across the wall changes, as shown in Fig. 7. The solar radiation hitting the external wall when reaches the PCM layer is used to melt the PCM which remains at its melting temperature as long as there is some solid PCM.

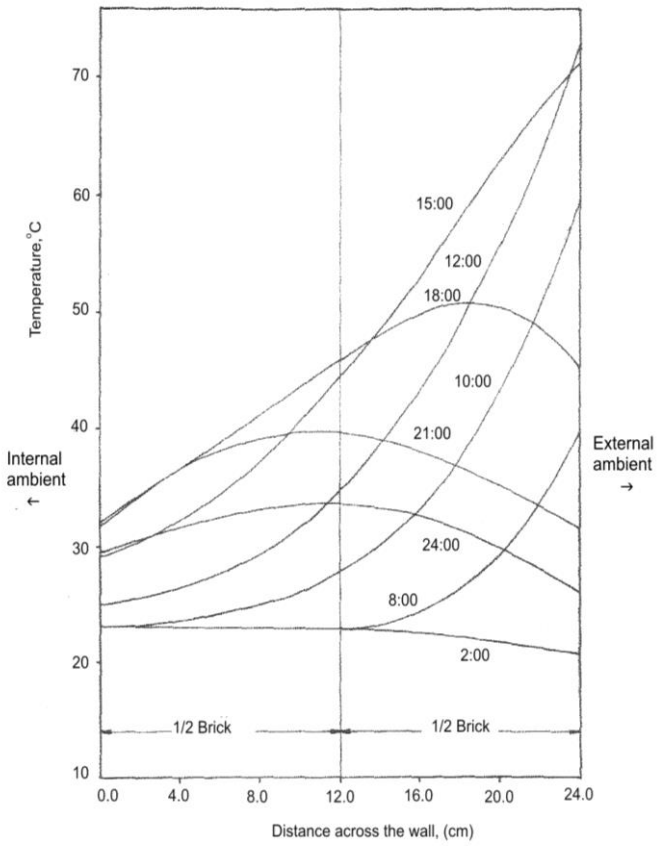

Fig. 6 Temperature profile across a section of a conventional wall.

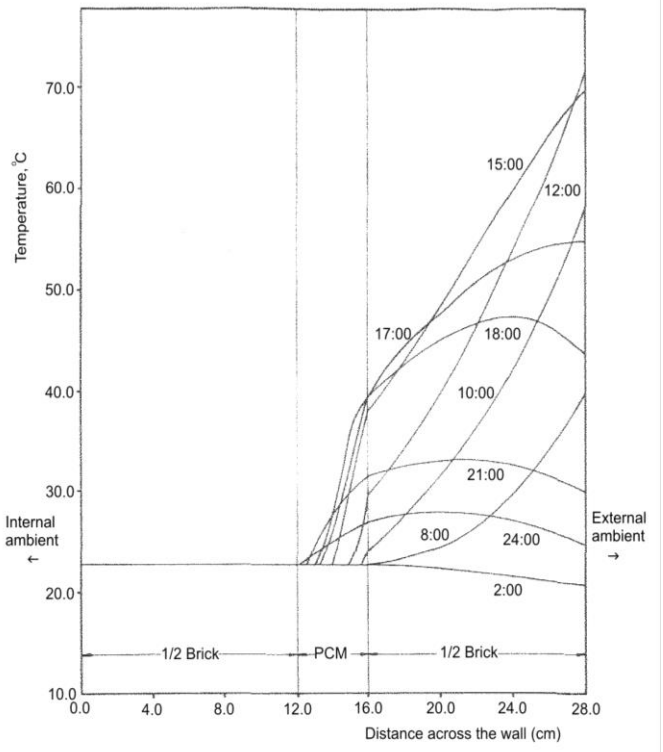

Fig. 7 Temperature profile across a section of a brick wall and PCM layer of 40.0 mm thickness.

In this way it acts as a thermal barrier against heat transferred from the external side of the wall. If the thickness of the PCM layer is calculated correctly (that is PCM does not melt completely until sunset), the internal ambient will not suffer any temperature change as a result of the heat transferred from the external wall. At night when the external temperature drops down, the external wall temperature will drop down and heat will be transferred from the melt PCM to the external ambient, without affecting the internal ambient temperature, until sun rise and the process is repeated.

Fig. 8 shows the case when the PCM thickness is smaller than the value necessary to perform thermal insulation in a full cycle.

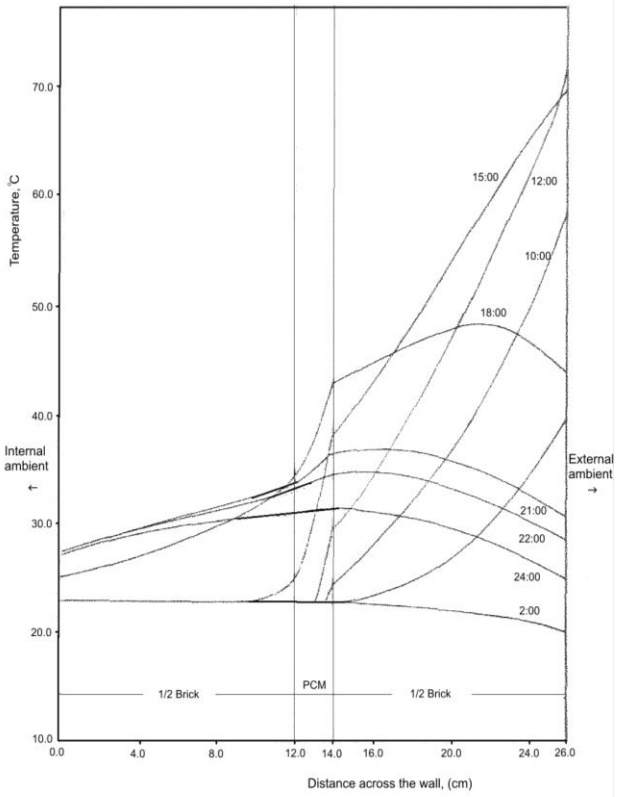

Fig. 8 Temperature profile across a section of a brick wall and PCM layer of 20.0 mm thickness.

In this situation all the PCM layer melts and its temperature starts to increase above the phase change temperature and consequently some heat is transferred to the internal ambient causing its temperature to increase. At night time when the external ambient temperature drops down the external wall temperature will decrease and heat will be transferred from the melt PCM to the external ambient until all the PCM is solidified. At this stage the heat transfer will continue from the internal ambient to the external ambient and gradually lowering the internal temperature.

Similar results and effects are found for the case of roof with and without PCM. The results are omitted for brevity.

In order to validate the numerical, the model and the predictions experiments were realized for the cases of wall and roof with and without PCM. The data from the experimental measurements were fed as entries to the simulation program.

Fig. 9 shows a comparison between the numerical prediction and the experiments for the internal and external wall temperatures. As can be seen, the agreement is reasonably good.

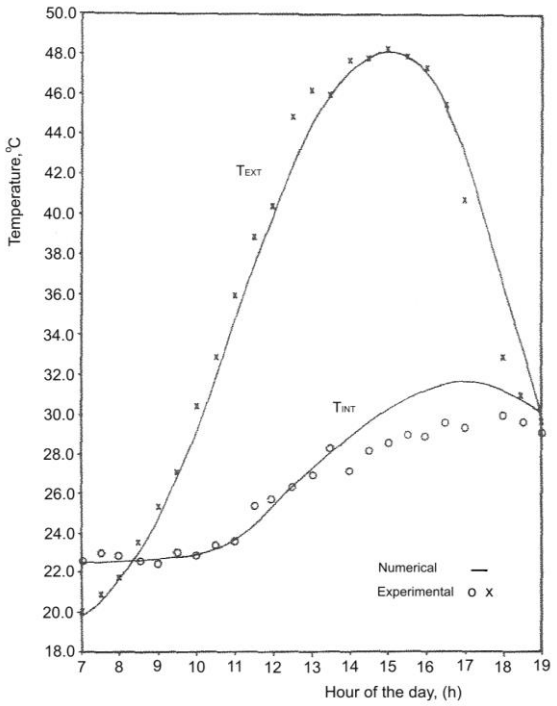

Fig. 9 Hourly variation of the numerical and experimental temperature of the external and internal faces of a conventional wall.

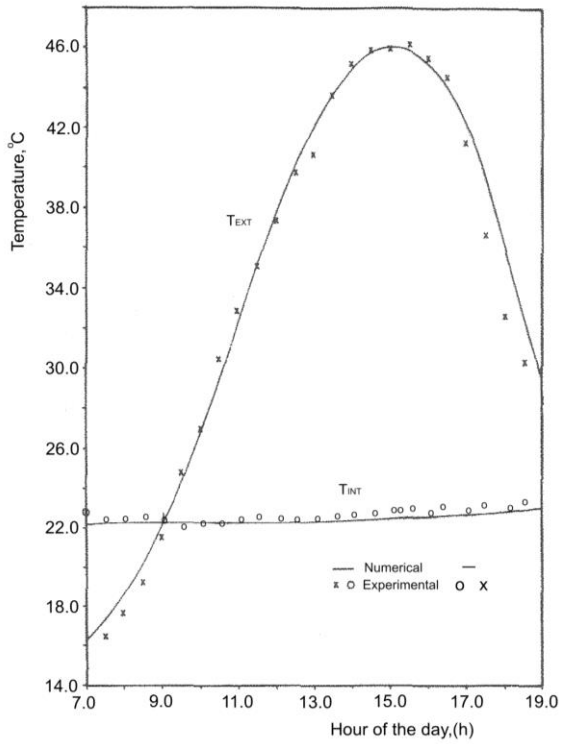

Fig.10 Hourly variation of the numerical and experimental temperature of the external and internal faces of a PCM wall.

Fig. 10 shows a comparison for the case of wall with PCM. As can be seen, the internal ambient temperature is maintained constant near the pre established value and the agreement between predictions and experiment is reasonably good.

The comparative results for the case of roofs without and with PCM are shown in Figs. 11 and 12. One can see the insulating effect due to the PCM layer.

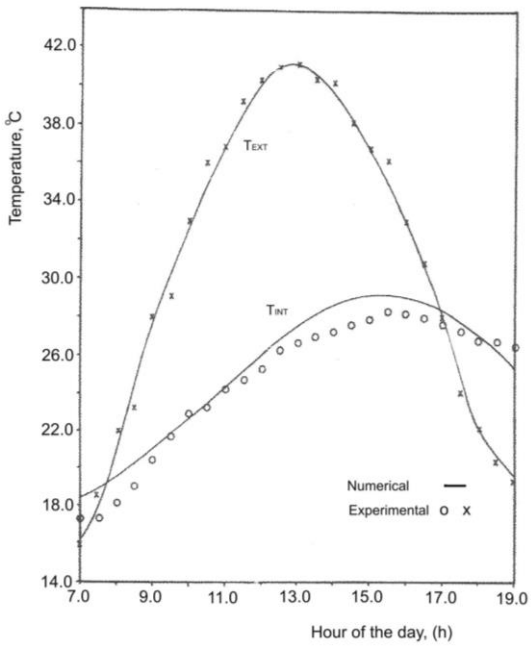

Fig. 11 Hourly variation of the numerical and experimental temperature of the external and internal faces of a conventional roof.

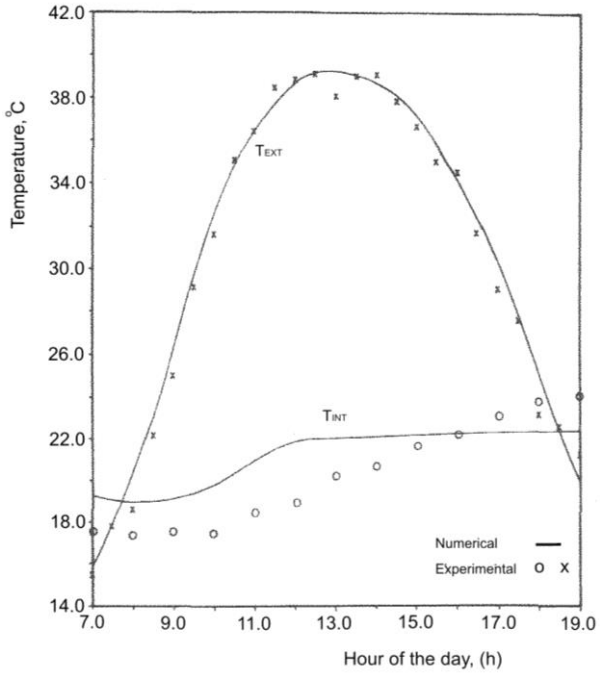

Fig. 12 Hourly variation of the numerical and experimental temperature of the external and internal faces of a PCM roof.

Fig. 13 shows a comparison between the numerical predictions and the experimental measurements of the transient variation of the temperature across a conventional wall. As can be seen, the increase of the external ambient temperature results in a corresponding increase of the internal ambient temperature, which can reach 29 ^{o}C as shown in Fig. 13.

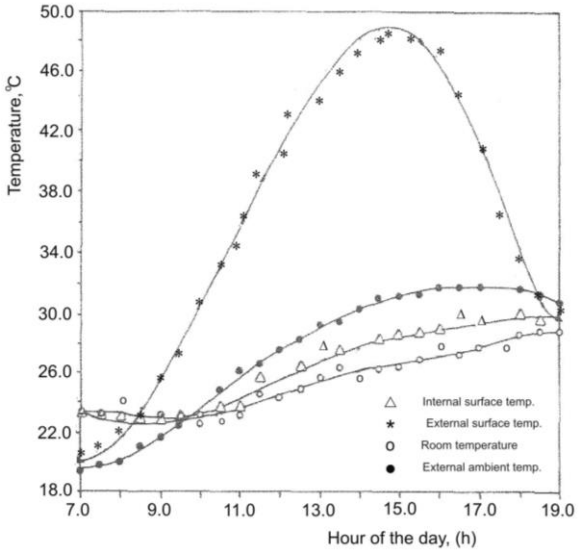

Fig. 13 Hourly variation of the external and internal surface temperatures of a conventional wall.

Fig. 14 is for a similar PCM wall and as one can observe, the presence of the PCM layer absorbs the heat conducted across the brick layer and melts the PCM. In this manner the internal ambient temperature is maintained constant at the phase change temperature. Observe that in this experiment the thickness of the PCM layer is 4 cm enough to cope with a full daily cycle without total melting or total solidification of the PCM layer.

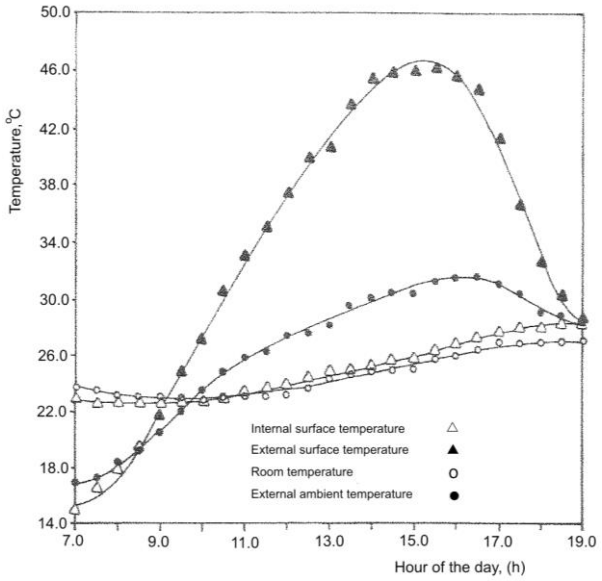

Fig. 14 Hourly variation of the external and internal surface temperatures of a brick wall with a PCM layer.

In the case of conventional and PCM roofs, similar results are found when comparing the temperature distribution across the roof's material.

Fig. 15 shows experimental temperature distribution on a conventional wall during a day. As can be seen, the increase of the temperature on the external side facing the sun is conducted with a time lag to the internal ambient. The difference in temperature at the contact region between the two walls is due to the imperfect contact between them.

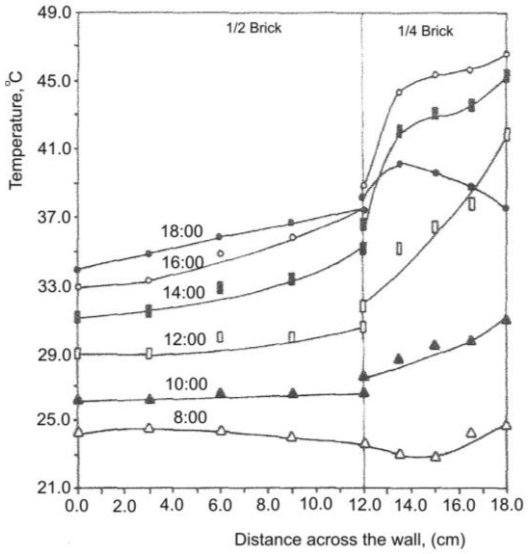

Fig. 15 Hourly variation of the external and internal temperatures across the thickness of a conventional wall.

Fig. 16 belongs to the same experiment and shows the transient variation of the internal and external ambient temperatures as well as the temperatures of the internal and external surfaces of the wall.

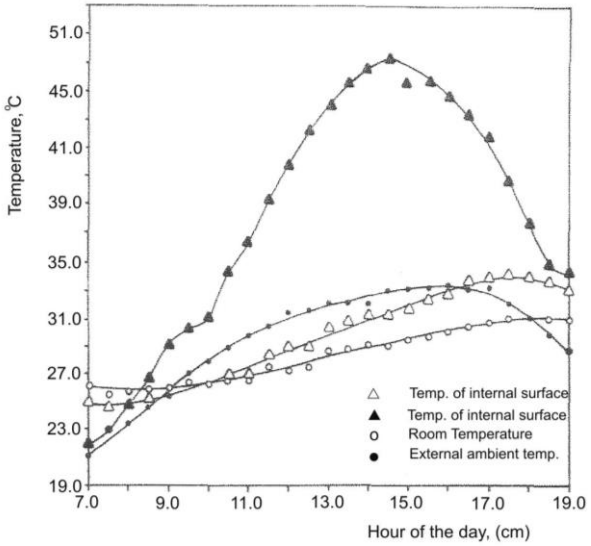

Fig. 16 Hourly variation of the external and internal temperatures of a conventional wall.

Fig. 17 shows the experimental variation of the temperature across the PCM wall during a day. As can be seen, the variation

of the external wall temperature is attenuated when passing through the PCM layer and a small amount is passed over to the internal ambient. In this experiment, the PCM layer is only 2 cm not enough for thermal insulation during a daily cycle. One can also observe a better thermal contact resistance because the PCM plastic bags soft and takes the shape of the space where they are inserted.

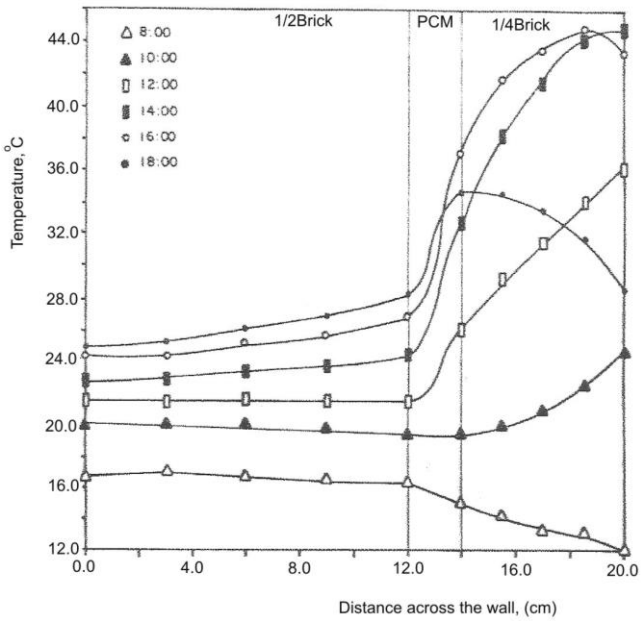

Fig. 17 Hourly variation of the external and internal temperatures across the thickness of a brick wall with PCM layer of 20.0 mm.

Fig. 18 shows the transient variation of the internal and external ambient temperatures as well as the temperatures of the internal and external surfaces of the wall.

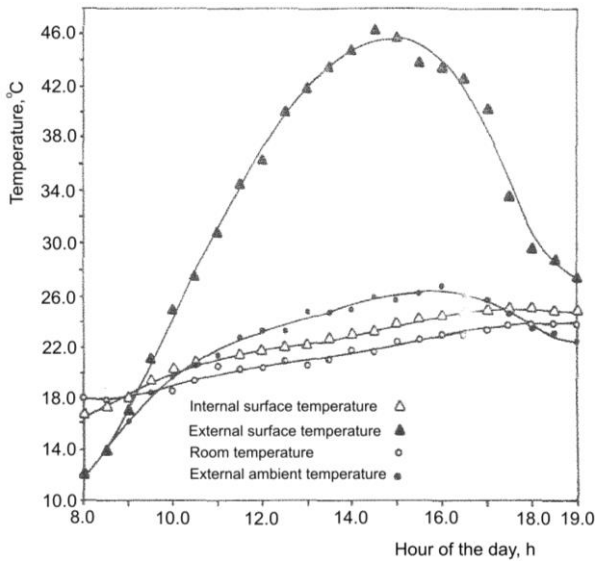

Fig. 18 Hourly variation of the external and internal temperatures of a brick wall with PCM layer.

Fig. 19 shows the temperature distribution across a PCM wall of 4 cm of PCM layer. The solar radiation incident on the external side of the wall passes through the PCM layer and is used to melt the PCM and hence maintains the temperature of the internal ambient nearly constant at the melting temperature.

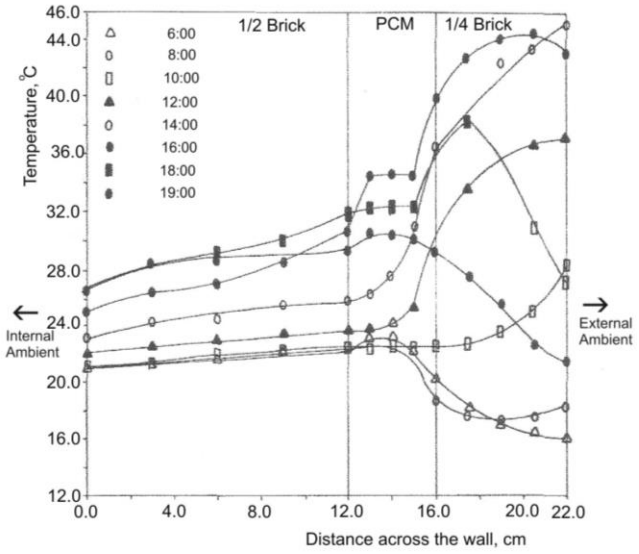

Fig. 19 Hourly temperature variation across a brick wall with a PCM layer of 40.0 mm thickness.

Fig. 20 shows the temperature variation across the conventional roof. When the external ambient temperature increases due to solar radiation, this causes a corresponding increase in the inner surface temperature reaching relatively high temperature.

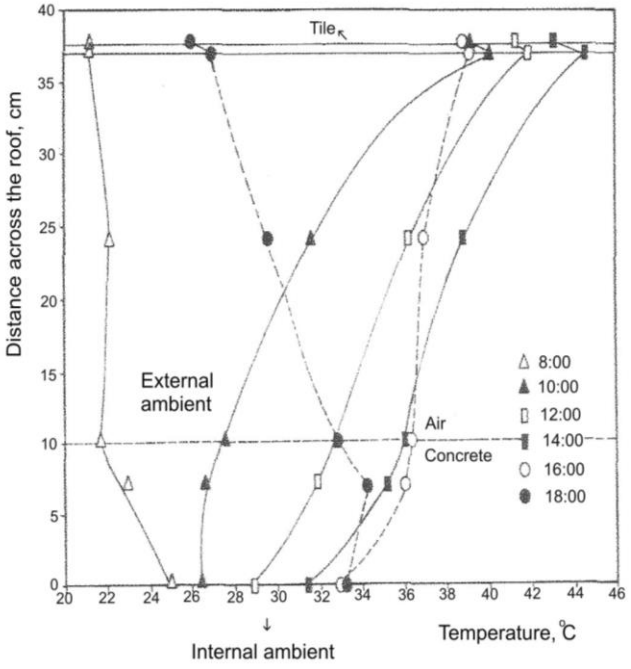

Fig. 20 Hourly temperature variation across a conventional roof.

The insertion of a PCM layer changes drastically the temperature in the internal ambient due to the fact that the PCM layer acts as shield against heat penetration into the internal ambient. The heat transferred across the PCM roof is used to melt the PCM and the temperature remains at the fusion temperature as long as there is a solid PCM as can be seen in Fig. 21.

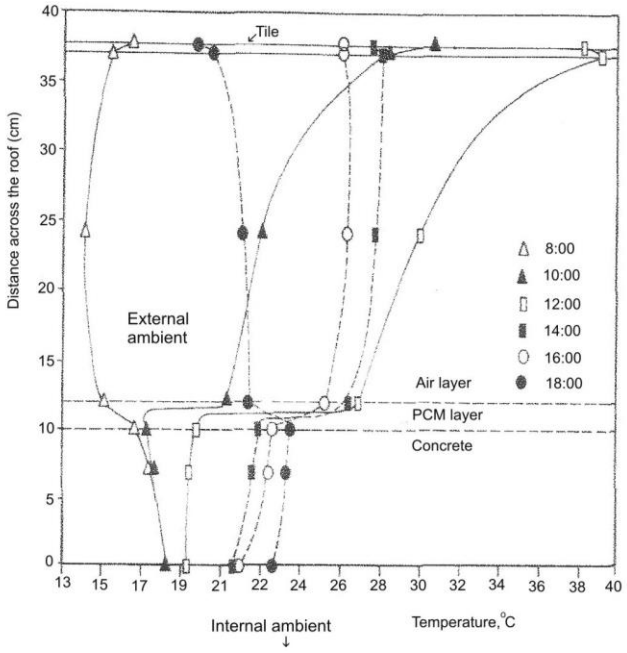

Fig. 21 Hourly temperature variation across a roof with a layer of PCM of 20.0 mm.

V. CONCLUSIONS

The results of this investigation reveal that the proposed model and its numerical predictions agree reasonably well with the experimental results and that the numerical model are capable of representing well the PCM wall and roof. It is confirmed experimentally that the PCM layer can reduce the heat gain, maintain the internal ambient temperature nearly constant and hence reduce the cooling load.

ACKNOWLEDGMENT

The first author wish to thank the CNPQ for the PQ research grant.

REFERENCES

[1] C. Bernard, Y. Body, A. Zanoli, "Experimental comparison of latent and sensible heat thermal walls", Solar Energy, Vol. 34, No. 6, 1985, pp. 475-487.

[2] K.A.R. Ismail, J.N.C. Castro, "PCM thermal insulation in buildings", Int. Journal of Energy Research, Vol. 21, 1977, pp. 1281-1296.

[3] A. Carbonari, M. De Grassi, C. Di Perna, P. Principi, "Numerical and experimental analyses of PCM containing sandwich panels for prefabricated walls", Energy and Buildings, Vol. 38, 2006, pp. 472–483.

[4] V. V. Tyagi, D. Buddhi, "PCM thermal storage in buildings: A state of art, Renewable and Sustainable Energy Reviews, Sustainability, Vol. 11, 2007, pp. 1146-1166.

[5] N. Zhu, Z. Ma, S. Wang, "Dynamic characteristics and energy performance of buildings using phase change materials: A review", Energy Conversion and Management, Vol. 50, 2009, pp. 3169–3181.

[6] M. H. M. Isa , X. Zhao, H. Yoshino, "Preliminary study of passive cooling strategy using a combination of PCM and copper foam to increase thermal heat storage in building Façade" , Sustainability, Vol. 2, 2010, pp. 2365-2381.

[7] F. Kuznik, D. David, K. Johannes, J. Roux, "A review on phase change materials integrated in building walls", Renewable and Sustainable Energy Reviews, Vol. 15, 2011, pp. 379–391.

[8] P. Hoes, M. Trcka, J.L.M. Hensen, B. H. Bonnema, "Investigating the potential of a novel low-energy house concept with hybrid adaptable thermal storage", Energy Conversion and Management, Vol. 52, 2011, pp. 2442–2447.

[9] M. Rostamizadeha, M. Khanlarkhani, S. M. Sadrameli, "Simulation of energy storage system with phase change material (PCM)", Energy and Buildings, Vol. 49, 2012, pp. 419–422.

[10] T. Silva, R. Vicente, N. Soares, V. Ferreira, "Experimental testing and numerical modeling of masonry wall solution with PCM incorporation: A passive construction solution", Energy and Buildings, Vol. 49, 2012, pp. 235–245.

[11] L. Zalewski , A. Joulin, S. Lassue, Y. Dutil, D. Rousse, "Experimental study of small-scale solar wall integrating phase change material", Solar Energy, Vol. 86, 2012, pp. 208–219.

[12] N. Soares, J.J. Costa, A.R. Gaspar, P. Santos, "Review of passive PCM latent heat thermal energy storage systems towards buildings' energy efficiency", Energy and Buildings, Vol. 59, 2013, pp. 82–103.

[13] M. Faraji, M.E. Alami, M. Najam, "Thermal Control of Building Using Latent Heat Storage South Wall", Journal of mathematics and computer science, Vol. 10, 2014, pp. 212-227.

[14] M. T. Chaichan, K. I. Abaas, "Performance amelioration of a Trombe wall by using Phase Change Material (PCM)", International Advanced Research Journal in Science, Engineering and Technology, Vol. 2, No. 4, 2015, April, DOI 10.17148/IARJSET.2015.2401.

[15] S. M. Sajjadian, J. Lewis, S. Sharple, "The potential of phase change materials to reduce domestic cooling energy loads for current and future UK climates", Energy and Buildings, Vol. 93, 2015, pp. 83–89.

[16] W. Saman, F. Bruno, E. Halawa, "Thermal performance of PCM thermal storage unit for a roof integrated solar heating system", Solar Energy, Vol. 78, 2005, pp. 341–349.

[17] A. Pasupathy, L. Athanasius, R. Velraj, R.V. Seeniraj, "Experimental investigation and numerical simulation analysis on the thermal performance of a building roof-incorporating phase change material (PCM) for thermal management", Applied Thermal Engineering, Vol. 28, 2008 pp. 556–565.

[18] H. J. Alqallaf, E. M. Alawadhi, "Concrete roof with cylindrical holes containing PCM to reduce the heat gain", Energy and Buildings, Vol. 61, 2013, pp. 73–80.

[19] H. Chou, C. Chen, V. Nguyen, "A new design of metal-sheet cool roof using PCM", Energy and Buildings, Vol. 57, 2013, pp. 42–50.

[20] S. Guichard, F. Miranville, D. Bigot, H. Boyer, "A thermal model for phase change materials in a building roof for a tropical and humid climate: Model description and elements of validation", Energy and Buildings, Vol. 70, 2014, pp. 71–80.

[21] A. Tokuç, T. Basaran, S. C. Yesügey, "An experimental and numerical investigation on the use of phase change materials in building elements: The case of a flat roof in Istanbul", Energy and Buildings, Vol. 102, 2015, pp. 91–104.

[22] H. C. Hottel, "A simple model for estimating the transmittance of direct solar radiation through clear atmospheres", Solar Energy, Vol. 18, 1976, pp.129-134.

[23] B. Y. H. Liu, R.C. Jordan, "The interrelations and characteristic distribution of direct, diffuse and total solar radiation", Solar Energy, Vol. 4, No. 3, 1960, pp.1-19.

[24] ASHRAE Handbook of Fundamentals, Chapter 27, "Fenestration". American Society of Heating, Refrigerating and Air-Conditioning Engineers, Inc., USA, 1993.

[25] W. D. Murray, F. Landis, "Numerical and machine solutions of transient heat-conduction problems involving melting or freezing". Part I – Method of Analysis Sample Solutions, Journal of Heat Transfer, Vol. 81c, 1959, pp. 108-112.

Kamal A.R. Ismail, Master degree in Mechanical Engineering, "Fluid Machinery" in 1967 and PhD, in Aeronautical Engineering in 1972 from Southampton University, UK. Full Professor in Mechanical Engineering since 1980. Was the head of the post-graduate school in mechanical engineering for more than 14 years, Dean of the Mechanical Engineering Faculty for four years, technical consultant for a good number of governmental establishments, private industry and others. Main research areas include Energy storage, Thermal Comfort, Heat transfer, Aerodynamics, Hydrodynamics and energy for isolated areas. Interested in Engineering education, innovative programs and experimental equipment for teaching engineering. Responsible for creating engineering courses in the areas of Energy, Aeronautical Engineering in the under graduate and post-graduate levels. Author of 22 books in different engineering subjects in the area of interest, over 350 articles in journals and specialized conferences and congresses, author of more than 85 research projects, reviewer for more than 20 scientific journals and member of the editorial boards of three international journals.

J.N. Castro, Master degree in Mechanical Engineering, Doctorate degree in Mechanical Engineering, Research areas heat transfer and Fluid Mechanics. Associate Professor at Unesp, Guaratinguetá, SP. Brazil.

Fátima A. M. Lino, Master degree in Energy Planning and PhD in Mechanical Engineering, Post-doctorate in Mechanical Engineering. Research areas of interest, Heat Transfer, Waste Management and Treatment, Waste-to-energy research. Co-author of 4 books in different engineering subjects in the area of interest, over 22 articles in scientific journals, six articles in specialized conferences and congresses and reviewer for 3 scientific journals.